Published in final edited form as:
Microvasc Res. 2014 November ; 0: 55–63. doi:10.1016/j.mvr.2014.06.006.

Imaging the lymphatic system

Lance L. Munn[*] and **Timothy P. Padera**[*]
Department of Radiation Oncology, Massachusetts General Hospital, Boston, MA, USA

Abstract

Visualization of the lymphatic system is clinically necessary during diagnosis or treatment of many conditions and diseases; it is used for identifying and monitoring lymphedema, for detecting metastatic lesions during cancer staging and for locating lymphatic structures so they can be spared during surgical procedures. Imaging lymphatic anatomy and function also plays an important role in experimental studies of lymphatic development and function, where spatial resolution and accessibility are better. Here, we review technologies for visualizing and imaging the lymphatic system for clinical applications. We then describe the use of lymphatic imaging in experimental systems as well as some of the emerging technologies for improving these methodologies.

Keywords

Imaging; Lymphatic vessels; Technologies; Lymph node; Lymphatic function; Lymphatic metastasis; Lymphography; Fluorescence; Models; Clinical

Introduction

The lymphatic system is responsible for maintaining proper tissue–fluid balance, organizing the immune system and absorbing lipids in the gut. It consists of the lymphatic vessels and lymph nodes through which lymph and immune cells traffic to establish and maintain immune responses. Therefore, disruption of lymphatic function results in lymph-edema—fluid accumulation in a tissue due to deficient lymphatic function—and local immuno-compromise, both of which lead to significant morbidity. The lymphatic system is also involved in cancer progression, as entry of metastatic cancer cells into the lymphatic system can result in lymph node metastases. Thus, the lymphatic system is central to a variety of pathological processes and many techniques have evolved to allow visualization of its anatomy and function (Rockson, 2003; Sevick-Muraca et al., 2014).

The lymphatic system consists of small lymphatic capillaries— termed initial lymphatics—that absorb interstitial fluid and cells to create lymph. These initial lymphatics bring lymph to the collecting lymphatic vessels, which are critical for transporting lymph over long distances through lymph nodes and eventually to the blood (Schmid-Schönbein, 1990). As opposed to the blood system, lymph flow is not always present, and is not driven by a

[*] Corresponding authors. lmunn@mgh.harvard.edu (L.L. Munn), tpadera@mgh.harvard.edu (T.P. Padera)..

central pump. This brings the possibilities of pathologies unique to the lymphatic system that generally manifest as problems with fluid homeostasis and the resulting edema. It also requires a different set of tools for diagnosis and analysis compared with the cardiovascular system.

In general, lymphatic vessels are difficult to visualize because they contain few cells, carrying mainly clear lymph fluid. This makes them difficult to locate and cannulate for angiographic techniques. Therefore, most visualization techniques rely on the natural ability of lymphatic vessels to absorb tracers injected into the tissue space. The tracer is then transported and concentrated into the proximal network, allowing detection by a variety of imaging modalities.

Imaging the lymphatic system in the clinic for assessment of function and diagnosis

Lymphography

Traditional lymphography and lymphangiography are natural extensions of angiography, a common method used to visualize the cardiovascular system by direct injection of a contrast agent into a vessel. One main difference is that intravascular contrast can be injected at any point in the cardiovascular system in order to highlight the entire blood vasculature. However, lymphatic contrast needs to be introduced in the periphery and will only highlight the lymphatic vessels draining that position. To identify a lymphatic vessel for cannulation, a contrast agent—such as Direct Blue or Patent Blue—is injected into the dermis where it is absorbed by initial lymphatics and fills the lymphatic vessels that drain the injection site. This allows identification of lymphatic channels that can then be cannulated and injected with an opaque contrast agent for radiographic imaging (Fig. 1A). Originally developed by Kinmonth (1952) as a guide during surgical procedures, lymphangiography has been modified and adapted for other diagnostic and experimental applications. The technique, which requires multiple injections into the tissue and microcannulation of vessels, is invasive and time consuming (Clement and Luciani, 2004; Halsell et al., 1965; Weissleder and Thrall, 1989) and has generally been supplanted by newer methods, described below.

Lymphoscintigraphy

Lymphoscintigraphy is a commonly-used imaging method in the clinic (Mihara et al., 2012; O'Mahony et al., 2004; Sevick-Muraca et al., 2014; Weissleder and Thrall, 1989; Wen et al., 2014) that relies on a radioactive tracer such as ^{99m}-technetium (^{99m}-Tc) being injected in the tissue (Kim et al., 2004b; Mieog et al., 2011; Ogasawara et al., 2008; Shih et al., 2001). As it drains through the lymphatic system, it can be imaged using a scintillation camera that integrates the signal over time to produce a 2D image of the lymphatic network (Fig. 1B). By repeated imaging of a lymph node over time, lymphatic drainage can be assessed by the increase in signal intensity over time. However, the poor resolution of this technique does not allow clear identification of vessel or lymph node location.

3D imaging is also possible with scintigraphy. Single-photon emission computed tomography (SPECT) uses triangulated information from multiple detectors to reconstruct

3D images of radioactive tracers (Barrett et al., 2006; Mar et al., 2007; O'Mahony et al., 2006). It is advantageous to add conventional x-ray CT to this method, to perform SPECT/CT, which localizes the lymphatic tracer at relatively low resolution (1–2 cm), but in relation to the high-resolution anatomy provided by the CT scan (Basu and Alavi, 2009; Tseng et al., 2014; Vermeeren et al., 2009). This method has proven useful in analysis of lymphatic drainage and sentinel lymph node identification in cases of head and neck melanoma (Mar et al., 2007), and diagnosis of primary intestinal lymphangiectasia (Wen et al., 2014), breast cancer (Basu and Alavi, 2009; Cheville et al., 2009; Spanu et al., 2011; Uren et al., 2012; Vercellino et al., 2014), multiple melanoma (Uren, 2009) and endometrial cancer (Sawicki et al., 2013).

Although one of the earliest techniques for imaging lymphatics and diagnosing lymphedema, scintigraphic methods are still used today. Nevertheless, lymphoscintigraphy carries many disadvantages, including the generally poor spatial resolution, the added expense when combined with CT, and the exposure to radioactive compounds by the patient and clinician, which necessitates special protection equipment and waste handling. For these reasons, other techniques have emerged to replace lymphoscintigraphy for many applications.

Magnetic resonance lymphography (MRL)

Magnetic resonance imaging relies on variations in T1 or T2 relaxation times when protons are in different tissue environments. It provides high contrast and good spatial resolution in soft tissues such as the lymphatic system, especially when extrinsic contrast agents are used (Fig. 1C). Ultrasmall super-paramagnetic iron oxide (USPIO, <50 nm) is a common contrast agent that decreases relaxation times in lymph nodes due to its specificity for the reticuloendothelial system (RES) present in normal nodes, but less prevalent in tumor containing nodes. This results in the focal, non-enhancing regions in lymph nodes with metastases (Harisinghani et al., 2005). Due to the negative-contrast nature of the detection, however, small lesions can be missed. The technique is relatively non-invasive and can be used to identify anatomic and physiological abnormalities associated with lymphatic dysfunction in order to determine further treatment strategies (Lohrmann et al., 2009). MRL has shown promise in imaging the lymphatic system in multiple pathologies including breast cancer (Lu et al., 2013), lymphedema (Lohrmann et al., 2007; Rane et al., 2013) and diffuse lymphangiomatosis (Lohrmann et al., 2011). Imaging agents with better sensitivity and specificity are under development (McDermott et al., 2013) and will improve the ability of MRL to identify pathologies in the lymphatic system.

The poor spatial resolution and sensitivity are limitations of MRL (Budiharto et al., 2011; Choi et al., 2006; Heck et al., 2014; Komatsu et al., 2005). Further improvements to the methodology, including new probes, show promise in increasing spatial resolution and the utility of this method (Kobayashi et al., 2004).

PET/CT

An important application of lymphography in the clinic involves screening lymph nodes for metastatic colonies. If large enough, these can be detected as abnormalities in the pattern of

tracer during lymphography or lymphoscintigraphy. Because smaller lesions are not always detected, other methods are often used for cancer staging. One such method is positron emission tomography (PET) (Birim et al., 2005). This takes advantage of the uptake of ^{18}fluorodeoxyglucose into the metabolically active cancer cells, which accumulate significant amounts of ^{18}F and can be detected in the nodes, even in low numbers. Again, however, the spatial resolution of this method is low, and it must be combined with other imaging modalities to clearly define the anatomy. Thus PET is often combined with CT scans during lymph node staging (Fig. 1D–F). Some studies have shown benefits of using PET/CT for lymph node staging (Choi et al., 2006; Mertens et al., 2013; Seo et al., 2014; Souillac et al., 2012; Takenaka et al., 2012; Uchiyama et al., 2012). However, the majority of reports conclude that PET/CT is not a reliable method due to false positives from inflammatory conditions (due to the metabolism of activated macrophage) and false negatives from limited sensitivity or spatial resolution (Akbulut et al., 2011; Al-Sarraf et al., 2008; Barranger et al., 2003; Bille et al., 2013; Chae et al., 2009; Cooper et al., 2011; Lovrics et al., 2004; Takamochi et al., 2005; Wagner et al., 2011; Xu et al., 2014). Because of these limitations, PET/CT results are normally combined with, or confirmed by, other methods.

Contrast-enhanced ultrasound (CEUS)

Conventional US creates tomographic images of tissue based on differences in reflection and diffraction of ultra high frequency sound waves. To be useful for lymphatic imaging, contrast enhancers—generally microbubbles consisting of gaseous cores enclosed in lipid or polymer shells—are injected, allowing visualization of lymph nodes as the microbubbles are disrupted by the applied acoustic waves. Specificity for lymph nodes comes from the fact that the microbubbles are phagocytosed by macrophages residing in the nodes. CEUS has shown promise in many studies (Abe et al., 2013; Kebudi et al., 2005; Yasufuku et al., 2006) and has proven useful in guiding the acquisition of fine-needle biopsies (Eloubeidi et al., 2005; Fujiwara et al., 2010; Lococo et al., 2012; Wada et al., 2010; Yasufuku et al., 2011).

Near-infrared (NIR) fluorescence imaging

Fluorescence imaging is an optical technique in which incident photons excite molecules in tissue, which then emit light (usually at a longer wavelength) as the electrons return to the ground state. Photodiode detectors or cameras attached to imaging systems record the resulting spatially-resolved signal (Fig. 1G–J). A limitation of optical imaging is the low penetration depth of light in tissue. This penetration is greatly attenuated as wavelength decreases, and depends greatly on the variable absorption and scattering properties of specific wavelengths in various tissues. Photons near the infrared range of the spectrum penetrate farther than those near the ultraviolet. Thus, with optics and detectors that operate in the near infrared, it is possible to obtain relatively high resolution images up to a few millimeters into soft tissues (Weiler et al., 2012). This requires fluorescent tracers that absorb and emit at near infrared wavelengths, generally in the 750–1000 nm range. ICG (indocyanine green) is such a fluorophore and has been used in the clinic for more than 50 years. It has significant overlap between absorption and emission bands, with absorption peak around 780–800 nm and emission at 810–830 nm. Thus, the excitation and detection system must be constructed to separate the emitted signal from the excitation light. Its

original applications—cardiac angiography and liver function analysis—often still use ICG today.

NIR imaging using ICG has recently been adopted for lymphography (Cahill et al., 2011; Mieog et al., 2011; Rasmussen et al., 2009; Sharma et al., 2008). ICG lymphography has been able to demonstrate the efficacy of manual lymphatic therapy in increasing lymph flow (Tan et al., 2011) and to detect early signs of lymphatic dysfunction in breast cancer survivors (Stout Gergich et al., 2008). Furthermore, ICG has been used to assess the extent and progression of lymphedema in patients (Aldrich et al., 2012). Studies have also shown feasibility and superiority of this method for sentinel node detection in breast cancer (Ogasawara et al., 2008; Polom et al., 2012; Sevick-Muraca et al., 2008; Tagaya et al., 2008; van der Vorst et al., 2012), vulvar cancer (Crane et al., 2011; Guo et al., 2014; Hutteman et al., 2012), cervical cancer (Jewell et al., 2014; van der Vorst et al., 2011), non-small cell lung cancer (Gilmore et al., 2012; Gilmore et al., 2013b), melanoma (Gilmore et al., 2013a; van der Vorst et al., 2013b), colorectal cancer (Cahill et al., 2011; van der Pas et al., 2013), and head and neck cancer (van der Vorst et al., 2013a). Even when the lymphatics or LNs are too deep to image non-invasively, it is possible to use minimally-invasive laparoscopy with a near IR detections system to perform the procedure (Cahill et al., 2011; Jewell et al., 2014; van der Pas et al., 2013). The technique does not require radiation exposure, provides relatively high resolution information in real time, and can be performed with equipment that is comparatively ergonomic and easily manipulated (Mieog et al., 2011). Currently, the main limitation is the depth of imaging.

Animal models of lymphatic function, development and metastasis

Many of the same techniques used in the clinic are applied in studies of the lymphatic system in animal models (Fukumura et al., 2010; Jain et al., 2002). These involve tissue injection of agents to provide contrast, which are imaged using one of the above methodologies. In many animal models, however, high resolution optical microscopy is used to visualize more details of the lymphatic vessels and lymph nodes. This provides valuable information about how lymphatic vessels form in development, how they drain fluid or actively pump, and how they convey metastatic or immune cells to lymph nodes. There is a rich literature using intravital microscopy to study cell trafficking and antigen transport in the lymph node (Mempel et al., 2004; Miller et al., 2002; Mora et al., 2003; Stoll et al., 2002; von Andrian, 1996). This impressive work generally focuses on immune cell behavior rather than lymphatic function, and is beyond the scope of this review. Animal models also provide platforms for testing new technologies before they are adopted in the clinic to help establish safety and efficacy (Gashev et al., 2010; Helle et al., 2012; Heuveling et al., 2012).

Development

Intravital microscopy has proved to be an important tool in understanding the development of the lymphatic system. Although many important steps in lymphatic system development were worked out in mouse models (Johnson et al., 2008; Srinivasan et al., 2007; Yang and Oliver, 2014), the use of zebrafish and xenopus models has allowed rapid interrogation of molecular lymphatic developmental pathways using intravital microscopy in these optically clear preparations (Ny et al., 2005; Yaniv et al., 2006). Studies by Yaniv et al. (2006) traced

the origin of cells that eventually constitute the thoracic duct in zebrafish. Studies in zebrafish and xenopus also show the developmental role of Notch/Dll4, COUP-TFII and synectin, in the lymphatic system (Fig. 2A–C) (Aranguren et al., 2011; Geudens et al., 2010; Hermans et al., 2010). These models will continue to build on our understanding of the molecular control of lymphatic development, particularly as new reporter animals are generated (Ny et al., 2013).

Analyses of lymph transport and lymphatic pumping

A major function of the lymphatic system is to drain excess fluid from tissue to maintain fluid homeostasis. Although seemingly straightforward, there is still much controversy over how lymph transport is achieved and regulated, especially in the context of pathologies such as cancer and lymphedema where fluid pressures and flows are altered. By imaging lymphatic vessels in animal models, many studies have addressed fundamental issues of lymph transport.

A basic question is how fluid pressures and velocities are related in tissues and their associated lymphatics. Swartz et al. used epifluorescence microscopy to track the movement of fluorescent tracers in the mouse tail after altering tissue fluid equilibrium by infusing saline into the tip of the tail. By careful fitting with a mathematical model, they were able to extract relationships between fluid drainage, tissue hydraulic conductivity and tissue swelling. They concluded that chronic swelling increases hydraulic conductivity, but the associated distension of tissue decreases the driving forces for fluid movement (Swartz et al., 1999).

Using the same mouse tail model with fluorescence lymphangiography, Leu et al. (2000) showed that sarcomas disrupt lymphatic vasculature and drainage patterns (Fig. 2D and E). Later, Hagendoorn et al. (2004) measured lymph flow rates after blocking nitric oxide synthase, and found that, rather than affecting flow in the initial lymphatic network, NOS activity was restricted to the underlying, collecting lymphatic vessels.

These collecting lymphatics are interesting because in addition to passive drainage, they can actively contract to drive fluid (Fig. 2F–H). How the contractions are initiated and regulated is an active area of research. Because these collecting lymphatic vessels lie deeper below the surface than the initial lymphatic networks, other models are generally required to observe and study this process. We have used mouse models to perform intravital microscopy of the afferent collecting lymphatic vessel to the popliteal lymph node in the mouse hindlimb. After surgically exposing the structures by removing the skin and overlying tissue, tracers such as FITC-dextran can be injected into the foot pad and visualized as they pass through the lymphatic vessels to the popliteal lymph node. This method allows for both the frequency and ejection fraction of lymphatic pumping to be measured (Liao et al., 2011). We have used this model to study the role of eNOS and iNOS in lymphatic pumping using mice genetically modified to lack these enzymes. We found that eNOS produced by the endothelium is necessary for normal lymphatic pumping, and that iNOS produced by Gr1+ myeloid cells during inflammation can produce excess NO that interferes with the pumping mechanism (Liao et al., 2011). Recently, a similar preparation combined with multiphoton fluorescence recovery after photobleaching techniques has been used to measure lymphatic

flow and the viscosity of lymph in vivo (Bouta et al., 2014). In conjunction with fluorescence tracers, multiphoton microscopy allows high resolution optical imaging of lymphatic structures. This has provided details of how tumor growth can affect lymphatic valves (Fig. 2I and J) (Hoshida et al., 2006).

Near infrared imaging has also been used to study lymphatic structure and function in animal models (Guo et al., 2009; Robinson et al., 2013). Using NIR imaging, lymphatic pumping frequency can be measured (Gogineni et al., 2013; Proulx et al., 2010) as well as maximum lymphatic pumping pressure and clearance rates (Bouta et al., 2014; Nelson et al., 2014). NIR imaging has also been used to distinguish phenotypic differences in mouse models of acute and chronic inflammation based on lymphatic function (Guo et al., 2009; Zhou et al., 2010) and abnormalities in the lymphatic system of Prox1-deficient mice (Kwon and Sevick-Muraca, 2011).

When more control over experimental conditions is desired, lymphatic vessels can be isolated and cannulated ex vivo in order to study the effects of pressure, flow, electrical stimulation or biochemical agents on the contractile behavior (Davis et al., 2008; Davis et al., 2012; Fox and von der Weid, 2002; Gashev et al., 2009; McHale and Roddie, 1976; McHale et al., 1988; Scallan et al., 2013; Zawieja et al., 2012). In general, images are acquired of the isolated vessel at 24 frames per second or faster, and parameters such as minimum and maximum diameters, contraction amplitude, contraction frequency and ejection fraction are measured by image analysis. These studies have established fundamental pressure/flow relationships in collecting lymphatic vessels and identified molecular regulators of lymphatic contraction (Davis et al., 2012; Gashev et al., 2002; Gasheva et al., 2006; von der Weid, 2013; Zawieja, 2009).

Models of lymph node metastasis

Animal models of cancer dissemination can be useful for studying the initial steps of metastasis. Such studies are most powerful when the cancer cells can be visualized intravitally over the time course of progression. When combined with existing animal models of tumor growth, lymphangiography allows studies of cancer-induced changes in the lymphatic vasculature, which alter the ability of the cancer to spread to lymph nodes.

When non-invasive imaging is not possible, surgical procedures expose or exteriorize lymphatic beds for visualization of the metastatic processes. Imaging fluorescently-labeled cancer cells through a skin flap preparation as they trafficked from the footpad of nude mice using intravital fluorescence, Hayashi et al. (2007) found that pressure applied to the tissue at the site of tumor growth increases metastasis.

Trauma to the tissue can introduce artifacts into an analysis of lymphatic function, especially in small animal models. Therefore, non-invasive methods are preferred. In some tissues, the lymphatic structures are sufficiently near the surface so that they can be studied using fluorescence microscopy in the visible range. For example, in the mouse ear, lymphatics can be observed after injection of FITC-dextran into the tip of the ear, revealing the drainage network through the ear that feeds into a large collecting vessel at the base of the ear and then the cervical lymph node (Jain et al., 2012). Using this technique after growing a

sarcoma near the tip of the ear, Hoshida et al. (2006) found that VEGF-C overexpression by cancer cells causes peritumor lymphatic hyperplasia and enhances lymph drainage from the ear. This also resulted in dramatic increases in the rates of metastatic cancer cells arriving in the cervical LN. Using similar methods, we showed that tumors have no functional lymphatic vessels, but that hyperplastic lymphatic vessels in the tumor margin are sufficient to increase metastatic spread to lymph nodes. The hyperplasia, induced by VEGF-C, creates more lymphatic surface area, which facilitates trans-lymphatic invasion from the tumor margin (Padera et al., 2002), with VEGF-C likely also altering the lymphatic endothelial cell biology to make them active partners in the metastatic process (Pepper et al., 2003). Later, we showed that compression of lymphatic vessels by the growing tumor was responsible for the lack of functional lymphatics within the tumor mass (Padera et al., 2004).

Intravital luminescence reporters can also be valuable tools for tracking cells in development: using a VEGFR3(EGFPLuc) mouse model, where an EGFP-luciferase fusion protein, expressed under the endogenous transcriptional control of the VEGFR3 gene, Martinez-Corral et al. (2012) were able to visualize tumor-induced lymphangiogenesis.

As in clinical analyses, near-infrared fluorescence imaging has advantages for preclinical studies. NIR imaging does not, in general, require surgical exposure of the lymphatic system, and has been used as a non-invasive imaging technique to study lymphatics in a variety of animal models. Using NIR imaging of ICG after injection of melanoma cells into the hindpaw, Kwon et al. (2013) were able to observe alterations in lymph drainage patterns, decreased lymphatic contractions and could identify metastases in the draining LNs that were responsible for these effects. Using a similar system with NIR imaging, Proulx and coworkers found that lymphatic vessels draining a melanoma grown in the footpad are dilated but functional, even though contraction rates decrease. Only after metastases developed in draining lymph nodes was flow disrupted, with lymph and cells redirected to other nodes (Fig. 2K and L) (Proulx et al., 2013a).

Emerging technologies

Each of the techniques described above has proven useful in some aspect of lymphatic research or clinical application. However, none is ideal, and recurring issues include poor spatial resolution, invasive procedures that impact patient comfort or alter lymphatic physiology, and potential chemical or radiation toxicity. Therefore, efforts continue to develop new and improved methodologies for imaging lymphatic vessels and lymph nodes. Some of the emerging technologies include novel contrast agents or probes and improved imaging techniques such as optical coherence tomography (OCT), optical frequency domain imaging (OFDI) and multispectral imaging.

OCT/OFDI

Optical frequency domain imaging (OFDI) relies on differences in light scattering properties of tissue to provide contrast. It can also detect Doppler frequency shifts in moving red blood cells in order to create vascular maps of the tissue (Vakoc et al., 2009). OFDI has superior depth penetration, allowing imaging to depths of a few millimeters and does not require exogenous contrast agents. It provides high resolution in three dimensions, and can be used

to distinguish many important anatomical features including blood and lymphatic vessels. In this technique, hypocellularity in the lymph results in low scattering intensity, providing high-contrast images of the networks. It is possible to detect lymphatic dilation at the periphery of tumors as well as cellular masses within the lymphatics (Fig. 3A–C). Furthermore, because no contrast agent is needed, multiple longitudinal observations are possible during tumor growth (Vakoc et al., 2009).

OCT has been used to follow the process of wound healing (Fig. 3D–G) (Yousefi et al., 2013), and to assess whole lymph nodes to determine whether they contain metastases (John et al., 2013). This technique may have clinical application in assessing nodal status of cancer patients in the operating room. Other techniques based on optical coherence tomography (OCT) include super-resolution optical microangiography and ultrahigh resolution optical microangiography. These label-free methods also take advantage of the low scattering of lymph fluid to produce high contrast images of the lymphatic system. A broadband supercontinuum light source, providing an axial resolution of 2.3 μm and lateral resolution of 5.8 μm, provides sufficient resolution to image the capillary vasculature and lymphatic vessels innervating microcircula-tory tissue beds (Zhi et al., 2012).

Novel probes/contrast agents

Although ICG has proven useful as a clinical imaging agent for more than 50 years, it has some disadvantages. For example, it is relatively unstable in solution, is not excluded from blood vessels, and may have unwanted effects on lymphatic physiology (Gashev et al., 2010). Thus, recent efforts have focused on improving the contrast agents used for NIR imaging. One approach to improving stability is to encapsulate ICG within liposomes; it has been shown that these liposomes can be visualized within lymph nodes and sensitivity is high enough to detect differences in flow due to the presence of metastases (Proulx et al., 2010). Another proposed agent for NIR imaging has been constructed by conjugating a cyclic albumin-binding domain (cABD) peptide to a near-infrared fluorophore (IRDye800CW). Designated cABD-IRDye800, the agent showed enhanced vascular uptake, retention, and fluorescence yield compared to ICG (Davies-Venn et al., 2012; Robinson et al., 2013).

Additional proposed imaging agents with high fluorescence intensity and improved stability include liposome-coated chlorophyll nanocomposites (Fan et al., 2012), PEG-conjugated IR probes (Proulx et al., 2013a), NIR-emitting polymer nanoprobes (Noh et al., 2012; Proulx et al., 2013b), bovine serum albumin conjugated with IRDye 680 (Wu et al., 2012), quantum dots with IR spectra (Kim et al., 2004a) and Alexa Fluor 680 conjugated to bombesin (AF680-BBN) (Cai et al., 2013). Other groups are developing probes that can be detected by multiple imaging modalities such as magnetic iron oxide nanoparticles conjugated with near infrared fluorophores that can be imaged by both magnetic resonance imaging and NIR (Zhou et al., 2013).

Another advance in lymphatic visualization is multispectral imaging. Made possible by the development of cadmium-selenium quantum dots (Qdots) and fluorescence imaging systems that can detect multiple wavelengths simultaneously, this technique allows, for example, simultaneous visualization of drainage from multiple lymphatic basins in real time (Kosaka

et al., 2009) and might be used to predict the route of cancer cell metastasis to the LNs (Kobayashi et al., 2007).

Conclusions

Our knowledge of the lymphatic system still lags behind that of the cardiovascular system, even though interest in its roles in normal and pathological processes has grown. Because fluid is absorbed locally into initial lymphatics that carry it to larger vessels, a single injection of contrast agent during lymphangiography only enhances a subset of the network, and signal is low or absent in many segments. Thus, more sensitive contrast agents or methods that rely on intrinsic contrast are needed. With implementation of new contrast agents, NIR imaging is poised to become a standard technique in the clinic. Further development should also allow new imaging techniques such as OCT and OFDI to be implemented in robust ergonomic imaging devices for non-invasive, contrast agent-free imaging.

Acknowledgments

This work was funded in part by National Institutes of Health grants R01CA149285 (LLM) and R00-CA137167, R21-AI097745 and DP2-OD008780 (TPP).

References

Abe H, et al. Accuracy of axillary lymph node staging in breast cancer patients: an observer-performance study comparison of MRI and ultrasound. Acad. Radiol. 2013; 20:1399–1404. [PubMed: 24119352]

Akbulut Z, et al. Is positron emission tomography reliable to predict post-chemotherapy retroperitoneal lymph node involvement in advanced germ cell tumors of the testis? Urol. J. 2011; 8:120–126. [PubMed: 21656470]

Aldrich MB, et al. Lymphatic abnormalities in the normal contralateral arms of subjects with breast cancer-related lymphedema as assessed by near-infrared fluorescent imaging. Biomed. Opt. Express. 2012; 3:1256–1265. [PubMed: 22741072]

Al-Sarraf N, et al. Lymph node staging by means of positron emission tomography is less accurate in non-small cell lung cancer patients with enlarged lymph nodes: analysis of 1,145 lymph nodes. Lung Cancer. 2008; 60:62–68. [PubMed: 17920724]

Aranguren XL, et al. Transcription factor COUP-TFII is indispensable for venous and lymphatic development in zebrafish and Xenopus laevis. Biochem. Biophys. Res. Commun. 2011; 410:121–126. [PubMed: 21641336]

Barranger E, et al. Evaluation of fluorodeoxyglucose positron emission tomography in the detection of axillary lymph node metastases in patients with early-stage breast cancer. Ann. Surg. Oncol. 2003; 10:622–627. [PubMed: 12839846]

Barrett T, et al. Imaging of the lymphatic system: new horizons. Contrast Media Mol. Imaging. 2006; 1:230–245. [PubMed: 17191764]

Basu S, Alavi A. Multifaceted role of lymphatic mapping by SPECT/CT hybrid imaging in the multimodality management of patients with cancer. Eur. J. Nucl. Med. Mol. Imaging. 2009; 36:1017–1018. [PubMed: 19387638]

Bille A, et al. Evaluation of integrated positron emission tomography and computed tomography accuracy in detecting lymph node metastasis in patients with adenocarcinoma vs squamous cell carcinoma. Eur. J. Cardiothorac. Surg. 2013; 43:574–579. [PubMed: 22689182]

Birim O, et al. Meta-analysis of positron emission tomographic and computed tomographic imaging in detecting mediastinal lymph node metastases in nonsmall cell lung cancer. Ann. Thorac. Surg. 2005; 79:375–382. [PubMed: 15620991]

Bouta EM, et al. In vivo quantification of lymph viscosity and pressure in lymphatic vessels and draining lymph nodes of arthritic joints in mice. J. Physiol. 2014; 592:1213–1223. [PubMed: 24421350]

Budiharto T, et al. Prospective evaluation of 11C-choline positron emission tomography/computed tomography and diffusion-weighted magnetic resonance imaging for the nodal staging of prostate cancer with a high risk of lymph node metastases. Eur. Urol. 2011; 60:125–130. [PubMed: 21292388]

Burnand KM, et al. Popliteal node visualization during standard pedal lymphoscintigraphy for a swollen limb indicates impaired lymph drainage. AJ. Am. J. Roentgenol. 2011; 197:1443–1448.

Cahill RA, et al. Near-infrared laparoscopy for real-time intra-operative arterial and lymphatic perfusion imaging. Colorectal Dis. 2011; 13(Suppl. 7):12–17. [PubMed: 22098511]

Cai QY, et al. Near-infrared fluorescence imaging of gastrin releasing peptide receptor targeting in prostate cancer lymph node metastases. Prostate. 2013; 73:842–854. [PubMed: 23280511]

Chae BJ, et al. Positron emission tomography-computed tomography in the detection of axillary lymph node metastasis in patients with early stage breast cancer. Jpn. J. Clin. Oncol. 2009; 39:284–289. [PubMed: 19318373]

Cheville AL, et al. A pilot study to assess the utility of SPECT/CT-based lymph node imaging to localize lymph nodes that drain the arm in patients undergoing treatment for breast cancer. Breast Cancer Res. Treat. 2009; 116:531–538. [PubMed: 19152027]

Choi HJ, et al. Comparison of the accuracy of magnetic resonance imaging and positron emission tomography/computed tomography in the presurgical detection of lymph node metastases in patients with uterine cervical carcinoma: a prospective study. Cancer. 2006; 106:914–922. [PubMed: 16411226]

Clement O, Luciani A. Imaging the lymphatic system: possibilities and clinical applications. Eur. Radiol. 2004; 14:1498–1507. [PubMed: 15007613]

Cooper KL, et al. Positron emission tomography (PET) for assessment of axillary lymph node status in early breast cancer: a systematic review and meta-analysis. Eur. J. Surg. Oncol. 2011; 37:187–198. [PubMed: 21269795]

Crane LM, et al. Intraoperative near-infrared fluorescence imaging for sentinel lymph node detection in vulvar cancer: first clinical results. Gynecol. Oncol. 2011; 120:291–295. [PubMed: 21056907]

Davies-Venn CA, et al. Albumin-binding domain conjugate for near-infrared fluorescence lymphatic imaging. Mol. Imaging Biol. 2012; 14:301–314. [PubMed: 21688052]

Davis MJ, et al. Modulation of lymphatic muscle contractility by the neuropeptide substance P. Am. J. Physiol. Heart Circ. Physiol. 2008; 295:H587–H597. [PubMed: 18539752]

Davis MJ, et al. Intrinsic increase in lymphangion muscle contractility in response to elevated afterload. Am. J. Physiol. Heart Circ. Physiol. 2012; 303:H795–H808. [PubMed: 22886407]

Eloubeidi MA, et al. Endoscopic ultrasound-guided fine needle aspiration of mediastinal lymph node in patients with suspected lung cancer after positron emission tomography and computed tomography scans. Ann. Thorac. Surg. 2005; 79:263–268. [PubMed: 15620955]

Fan L, et al. Near infrared fluorescent chlorophyll nanoscale liposomes for sentinel lymph node mapping. Int. J. Nanomedicine. 2012; 7:3071–3080. [PubMed: 22787402]

Fortuin A, et al. Molecular and functional imaging for detection of lymph node metastases in prostate cancer. Int. J. Mol. Sci. 2013; 14:13842–13875. [PubMed: 23823804]

Fox JL, von der Weid PY. Effects of histamine on the contractile and electrical activity in isolated lymphatic vessels of the guinea-pig mesentery. Br. J. Pharmacol. 2002; 136:1210–1218. [PubMed: 12163355]

Fujiwara T, et al. The utility of sonographic features during endobronchial ultrasound-guided transbronchial needle aspiration for lymph node staging in patients with lung cancer: a standard endobronchial ultrasound image classification system. Chest. 2010; 138:641–647. [PubMed: 20382710]

Fukumura D, et al. Tumor microvasculature and microenvironment: novel insights through intravital imaging in pre-clinical models. Microcirculation. 2010; 17:206–225. [PubMed: 20374484]

Gashev AA, et al. Inhibition of the active lymph pump by flow in rat mesenteric lymphatics and thoracic duct. J. Physiol. 2002; 540:1023–1037. [PubMed: 11986387]

Gashev AA, et al. Methods for lymphatic vessel culture and gene transfection. Microcirculation. 2009; 16:615–628. [PubMed: 19626551]

Gashev AA, et al. Indocyanine green and lymphatic imaging: current problems. Lymphat. Res. Biol. 2010; 8:127–130. [PubMed: 20583875]

Gasheva OY, et al. Contraction-initiated NO-dependent lymphatic relaxation: a self-regulatory mechanism in rat thoracic duct. J. Physiol. 2006; 575:821. [PubMed: 16809357]

Geudens I, et al. Role of delta-like-4/Notch in the formation and wiring of the lymphatic network in zebrafish. Arterioscler. Thromb. Vasc. Biol. 2010; 30:1695–1702. [PubMed: 20466977]

Gilmore DM, et al. Developing intrathoracic sentinel lymph node mapping with near-infrared fluorescent imaging in non-small cell lung cancer. J. Thorac. Cardiovasc. Surg. 2012; 144:S80–S84. [PubMed: 22726707]

Gilmore DM, et al. Effective low-dose escalation of indocyanine green for near-infrared fluorescent sentinel lymph node mapping in melanoma. Ann. Surg. Oncol. 2013a; 20:2357–2363. [PubMed: 23440551]

Gilmore DM, et al. Identification of metastatic nodal disease in a phase 1 dose-escalation trial of intraoperative sentinel lymph node mapping in non-small cell lung cancer using near-infrared imaging. J. Thorac. Cardiovasc. Surg. 2013b; 146:562–570. (discussion 569–70). [PubMed: 23790404]

Gogineni A, et al. Inhibition of VEGF-C modulates distal lymphatic remodeling and secondary metastasis. PLoS One. 2013; 8:e68755. [PubMed: 23874750]

Guermazi A, et al. Lymphography: an old technique retains its usefulness. Radiographics. 2003; 23:1541–1558. (discussion 1559–60). [PubMed: 14615563]

Guo R, et al. Inhibition of lymphangiogenesis and lymphatic drainage via vascular endothelial growth factor receptor 3 blockade increases the severity of inflammation in a mouse model of chronic inflammatory arthritis. Arthritis Rheum. 2009; 60:2666–2676. [PubMed: 19714652]

Guo W, et al. Breast cancer sentinel lymph node mapping using near-infrared guided indocyanine green in comparison with blue dye. Tumour Biol. 2014; 35:3073–3078. [PubMed: 24307620]

Hagendoorn J, et al. Endothelial Nitric Oxide Synthase Regulates Microlymphatic Flow via Collecting Lymphatics. Circ. Res. 2004; 95:204. [PubMed: 15192027]

Halsell JT, et al. Lymphatic Drainage of the Breast Demonstrated by Vital Dye Staining and Radiography. Ann. Surg. 1965; 162:221–226. [PubMed: 14327002]

Harisinghani MG, et al. A pilot study of lymphotrophic nanoparticle-enhanced magnetic resonance imaging technique in early stage testicular cancer: a new method for noninvasive lymph node evaluation. Urology. 2005; 66:1066–1071. [PubMed: 16286125]

Hayashi K, et al. Real-time imaging of tumor-cell shedding and trafficking in lymphatic channels. Cancer Res. 2007; 67:8223–8228. [PubMed: 17804736]

Heck MM, et al. Prospective comparison of computed tomography, diffusion-weighted magnetic resonance imaging and [(11)C]choline positron emission tomography/computed tomography for preoperative lymph node staging in prostate cancer patients. Eur. J. Nucl. Med. Mol. Imaging. 2014; 41:694–701. [PubMed: 24297503]

Helle M, et al. Visualisation of sentinel lymph node with indium-based near infrared emitting Quantum Dots in a murine metastatic breast cancer model. PLoS One. 2012; 7:e44433. [PubMed: 22952979]

Hermans K, et al. Role of synectin in lymphatic development in zebrafish and frogs. Blood. 2010; 116:3356–3366. [PubMed: 20631376]

Heuveling DA, et al. Nanocolloidal albumin-IRDye 800CW: a near-infrared fluorescent tracer with optimal retention in the sentinel lymph node. Eur. J. Nucl. Med. Mol. Imaging. 2012; 39:1161–1168. [PubMed: 22349719]

Hoshida T, et al. Imaging steps of lymphatic metastasis reveals that vascular endothelial growth factor-C increases metastasis by increasing delivery of cancer cells to lymph nodes: therapeutic implications. Cancer Res. 2006; 66:8065–8075. [PubMed: 16912183]

Hutteman M, et al. Optimization of near-infrared fluorescent sentinel lymph node mapping for vulvar cancer. Am. J. Obstet. Gynecol. 2012; 206(89):e1–e5. [PubMed: 21963099]

Jain RK, et al. Dissecting tumour pathophysiology using intravital microscopy. Nat. Rev. Cancer. 2002; 2:266–276. [PubMed: 12001988]

Jain RK, et al. Lymphangiography of the mouse ear. Cold Spring Harb. Protoc. 2012; 2012:1179–1180. [PubMed: 23118365]

Jewell EL, et al. Detection of sentinel lymph nodes in minimally invasive surgery using indocyanine green and near-infrared fluorescence imaging for uterine and cervical malignancies. Gynecol. Oncol. 2014; 133:274–277. [PubMed: 24582865]

John R, et al. Three-dimensional optical coherence tomography for optical biopsy of lymph nodes and assessment of metastatic disease. Ann. Surg. Oncol. 2013; 20:3685–3693. [PubMed: 22688663]

Johnson NC, et al. Lymphatic endothelial cell identity is reversible and its maintenance requires Prox1 activity. Genes Dev. 2008; 22:3282–3291. [PubMed: 19056883]

Kebudi A, et al. The role of pre-operative B mode ultrasound in the evaluation of the axillary lymph node metastases in the initial staging of breast carcinoma. Acta Chir. Belg. 2005; 105:511–514. [PubMed: 16315836]

Kim S, et al. Near-infrared fluorescent type II quantum dots for sentinel lymph node mapping. Nat. Biotechnol. 2004a; 22:93–97. [PubMed: 14661026]

Kim SH, et al. Reverse echelon node and a lymphatic ectasia in the same patient during breast lymphoscintigraphy: the importance of injection and imaging technique. Br. J. Radiol. 2004b; 77:1053–1056. [PubMed: 15569651]

Kinmonth JB. Lymphangiography in man; a method of outlining lymphatic trunks at operation. Clin. Sci. (Lond.). 1952; 11:13–20. [PubMed: 14896514]

Kobayashi H, et al. Lymphatic drainage imaging of breast cancer in mice by micro-magnetic resonance lymphangiography using a nano-size paramagnetic contrast agent. J. Natl. Cancer Inst. 2004; 96:703–708. [PubMed: 15126607]

Kobayashi H, et al. Simultaneous multicolor imaging of five different lymphatic basins using quantum dots. Nano Lett. 2007; 7:1711–1716. [PubMed: 17530812]

Komatsu S, et al. Predictive value of the time-intensity curves on dynamic contrast-enhanced magnetic resonance imaging for lymphatic spreading in breast cancer. Surg. Today. 2005; 35:720–724. [PubMed: 16133665]

Kosaka N, et al. In vivo real-time, multicolor, quantum dot lymphatic imaging. J. Invest. Dermatol. 2009; 129:2818–2822. [PubMed: 19536144]

Kwon S, Sevick-Muraca EM. Mouse phenotyping with near-infrared fluorescence lymphatic imaging. Biomed. Opt. Express. 2011; 2:1403–1411. [PubMed: 21698004]

Kwon S, et al. Direct visualization of changes of lymphatic function and drainage pathways in lymph node metastasis of B16F10 melanoma using near-infrared fluorescence imaging. Biomed. Opt. Express. 2013; 4:967–977. [PubMed: 23761026]

Leu AJ, et al. Absence of functional lymphatics within a murine sarcoma: a molecular and functional evaluation. Cancer Res. 2000; 60:4324–4327. [PubMed: 10969769]

Liao S, et al. Impaired lymphatic contraction associated with immunosuppression. PNAS. 2011; 108:18784. [PubMed: 22065738]

Lococo F, et al. Transesophageal endoscopic ultrasound-guided transcarotid fine needle aspiration of a positron emission tomography (PET)-positive mediastinal lymph node. Endoscopy. 2012; 44(Suppl. 2 UCTN):E402–E403. [PubMed: 23169036]

Lohrmann C, et al. Magnetic resonance imaging of lymphatic vessels without image subtraction: a practicable imaging method for routine clinical practice? J. Comput. Assist. Tomogr. 2007; 31:303–308. [PubMed: 17414770]

Lohrmann C, et al. MR imaging of the lymphatic system in patients with lipedema and lipo-lymphedema. Microvasc. Res. 2009; 77:335–339. [PubMed: 19323976]

Lohrmann C, et al. Assessment of the lymphatic system in patients with diffuse lymphangiomatosis by magnetic resonance imaging. Eur. J. Radiol. 2011; 80:576–581. [PubMed: 19913379]

Lovrics PJ, et al. A prospective evaluation of positron emission tomography scanning, sentinel lymph node biopsy, and standard axillary dissection for axillary staging in patients with early stage breast cancer. Ann. Surg. Oncol. 2004; 11:846–853. [PubMed: 15313737]

Lu Q, et al. MR lymphography of lymphatic vessels in lower extremity with gynecologic oncology-related lymphedema. PLoS One. 2012; 7:e50319. [PubMed: 23209708]

Lu Q, et al. Imaging lymphatic system in breast cancer patients with magnetic resonance lymphangiography. PLoS One. 2013; 8:e69701. [PubMed: 23861979]

Mar MV, et al. Evaluation and localization of lymphatic drainage and sentinel lymph nodes in patients with head and neck melanomas by hybrid SPECT/CT lymphoscintigraphic imaging. J. Nucl. Med. Technol. 2007; 35:10–16. (quiz 17–20). [PubMed: 17337652]

Martinez-Corral I, et al. In vivo imaging of lymphatic vessels in development, wound healing, inflammation, and tumor metastasis. Proc. Natl. Acad. Sci. U. S. A. 2012; 109:6223–6228. [PubMed: 22474390]

McDermott S, et al. Accurate prediction of nodal status in preoperative patients with pancreatic ductal adenocarcinoma using next-gen nanoparticle. Transl. Oncol. 2013; 6:670–675. [PubMed: 24466369]

McHale N, Roddie I. The effect of transmural pressure on pumping activity in isolated bovine lymphatic vessels. J. Physiol. 1976; 261:255–269. [PubMed: 988184]

McHale NG, et al. Transient excitatory responses to sustained stimulation of intramural nerves in isolated bovine lymphatic vessels. Q. J. Exp. Physiol. 1988; 73:175–182. [PubMed: 3380933]

Mempel TR, et al. T-cell priming by dendritic cells in lymph nodes occurs in three distinct phases. Nature. 2004; 427:154–159. [PubMed: 14712275]

Mertens LS, et al. FDG-positron emission tomography/computerized tomography for monitoring the response of pelvic lymph node metastasis to neoadjuvant chemo-therapy for bladder cancer. J. Urol. 2013; 189:1687–1691. [PubMed: 23142689]

Mieog JS, et al. Toward optimization of imaging system and lymphatic tracer for near-infrared fluorescent sentinel lymph node mapping in breast cancer. Ann. Surg. Oncol. 2011; 18:2483–2491. [PubMed: 21360250]

Mihara M, et al. Low-invasive lymphatic surgery and lymphatic imaging for completely healed intractable pudendal lymphorrhea after gynecologic cancer treatment. J. Minim. Invasive Gynecol. 2012; 19:658–662. [PubMed: 22935310]

Miller MJ, et al. Two-photon imaging of lymphocyte motility and antigen response in intact lymph node. Science. 2002; 296:1869–1873. [PubMed: 12016203]

Mora JR, et al. Selective imprinting of gut-homing T cells by Peyer's patch dendritic cells. Nature. 2003; 424:88–93. [PubMed: 12840763]

Nelson TS, et al. Minimally invasive method for determining the effective lymphatic pumping pressure in rats using near-infrared imaging. Am. J. Physiol. Regul. Integr. Comp. Physiol. 2014; 306:R281–R290. [PubMed: 24430884]

Noh YW, et al. Near-infrared emitting polymer nanogels for efficient sentinel lymph node mapping. ACS Nano. 2012; 6:7820–7831. [PubMed: 22862428]

Ny A, et al. A genetic Xenopus laevis tadpole model to study lymphangiogenesis. Nat. Med. 2005; 11:998–1004. [PubMed: 16116431]

Ny A, et al. A transgenic Xenopus laevis reporter model to study lymphangiogenesis. Biol. Open. 2013; 2:882–890. [PubMed: 24143274]

Ogasawara Y, et al. Evaluation of breast lymphatic pathways with indocyanine green fluorescence imaging in patients with breast cancer. World J. Surg. 2008; 32:1924–1929. [PubMed: 18330628]

O'Mahony S, et al. Finding an optimal method for imaging lymphatic vessels of the upper limb. Eur. J. Nucl. Med. Mol. Imaging. 2004; 31:555–563. [PubMed: 14722673]

O'Mahony S, et al. Imaging of lymphatic vessels in breast cancer-related lymphedema: intradermal versus subcutaneous injection of 99mTc-immunoglobulin. AJ. Am. J. Roentgenol. 2006; 186:1349–1355.

Padera TP, et al. Lymphatic metastasis in the absence of functional intratumor lymphatics. Science. 2002; 296:1883–1886. [PubMed: 11976409]

Padera TP, et al. Pathology: cancer cells compress intratumour vessels. Nature. 2004; 427:695. [PubMed: 14973470]

Pepper MS, et al. Lymphangiogenesis and tumor metastasis. Cell Tissue Res. 2003; 314:167–177. [PubMed: 12883995]

Polom K, et al. Breast cancer sentinel lymph node mapping using near infrared guided indocyanine green and indocyanine green–human serum albumin in comparison with gamma emitting radioactive colloid tracer. Eur. J. Surg. Oncol. 2012; 38:137–142. [PubMed: 22130469]

Proulx ST, et al. Quantitative imaging of lymphatic function with liposomal indocyanine green. Cancer Res. 2010; 70:7053–7062. [PubMed: 20823159]

Proulx ST, et al. Use of a PEG-conjugated bright near-infrared dye for functional imaging of rerouting of tumor lymphatic drainage after sentinel lymph node metastasis. Biomaterials. 2013a; 34:5128–5137. [PubMed: 23566803]

Proulx ST, et al. Expansion of the lymphatic vasculature in cancer and inflammation: new opportunities for in vivo imaging and drug delivery. J. Control. Release. 2013b; 172:550–557. [PubMed: 23665257]

Rane S, et al. Clinical feasibility of noninvasive visualization of lymphatic flow with principles of spin labeling MR imaging: implications for lymphedema assessment. Radiology. 2013; 269:893–902. [PubMed: 23864103]

Rasmussen JC, et al. Lymphatic imaging in humans with near-infrared fluorescence. Curr. Opin. Biotechnol. 2009; 20:74–82. [PubMed: 19233639]

Robinson HA, et al. Non-invasive optical imaging of the lymphatic vasculature of a mouse. J. Vis. Exp. 2013:e4326. [PubMed: 23524658]

Rockson SG. Lymphatic investigation: from the endothelium to in vivo imaging. Lymphat. Res. Biol. 2003; 1:99. [PubMed: 19642943]

Sawicki S, et al. Preoperative detection of sentinel lymph nodes in endometrial cancer using SPECT/CT. Clin. Nucl. Med. 2013; 38:726–729. [PubMed: 23797222]

Scallan JP, et al. Constriction of isolated collecting lymphatic vessels in response to acute increases in downstream pressure. J. Physiol. 2013; 591:443–459. [PubMed: 23045335]

Schmid-Schönbein GW. Microlymphatics and lymph flow. Physiol. Rev. 1990; 70:987. [PubMed: 2217560]

Seo MJ, et al. Detection of internal mammary lymph node metastasis with (18)F-fluorodeoxyglucose positron emission tomography/computed tomography in patients with stage III breast cancer. Eur. J. Nucl. Med. Mol. Imaging. 2014; 41:438–445. [PubMed: 24196918]

Sevick-Muraca EM, et al. Imaging of lymph flow in breast cancer patients after microdose administration of a near-infrared fluorophore: feasibility study. Radiology. 2008; 246:734–741. [PubMed: 18223125]

Sevick-Muraca EM, et al. Emerging lymphatic imaging technologies for mouse and man. J. Clin. Invest. 2014; 124:905–914. [PubMed: 24590275]

Sharma R, et al. New horizons for imaging lymphatic function. Ann. N. Y. Acad. Sci. 2008; 1131:13–36. [PubMed: 18519956]

Shih WJ, et al. Lymphoscintigraphy of melanoma: lymphatic channel activity guides localization of sentinel lymph nodes, and gamma camera imaging/counting confirms presence of radiotracer in excised nodes. Ann. Nucl. Med. 2001; 15:1–11. [PubMed: 11355775]

Souillac I, et al. Prospective evaluation of (18)F-fluorodeoxyglucose positron emission tomography-computerized tomography to assess inguinal lymph node status in invasive squamous cell carcinoma of the penis. J. Urol. 2012; 187:493–497. [PubMed: 22177157]

Spanu A, et al. The usefulness of Tc-99 m-tetrofosmin SPECT/CT in the detection of residual tumors and axillary lymph node metastases in breast cancer patients following neoadjuvant therapy. Clin. Nucl. Med. 2011; 36:997–1002. [PubMed: 21975387]

Srinivasan RS, et al. Lineage tracing demonstrates the venous origin of the mammalian lymphatic vasculature. Genes Dev. 2007; 21:2422–2432. [PubMed: 17908929]

Stoll S, et al. Dynamic imaging of T cell-dendritic cell interactions in lymph nodes. Science. 2002; 296:1873–1876. [PubMed: 12052961]

Stout Gergich NL, et al. Preoperative assessment enables the early diagnosis and successful treatment of lymphedema. Cancer. 2008; 112:2809–2819. [PubMed: 18428212]

Swartz MA, et al. Mechanics of interstitial-lymphatic fluid transport: theoretical foundation and experimental validation. J. Biomech. 1999; 32:1297–1307. [PubMed: 10569708]

Tagaya N, et al. Intraoperative identification of sentinel lymph nodes by near-infrared fluorescence imaging in patients with breast cancer. Am. J. Surg. 2008; 195:850–853. [PubMed: 18353274]

Takamochi K, et al. Pitfalls in lymph node staging with positron emission tomography in non-small cell lung cancer patients. Lung Cancer. 2005; 47:235–242. [PubMed: 15639722]

Takenaka T, et al. Prediction of true-negative lymph node metastasis in clinical IA non-small cell lung cancer by measuring standardized uptake values on positron emission tomography. Surg. Today. 2012; 42:934–939. [PubMed: 22864936]

Tan IC, et al. Assessment of lymphatic contractile function after manual lymphatic drainage using near-infrared fluorescence imaging. Arch. Phys. Med. Rehabil. 2011; 92:756–764. e1. [PubMed: 21530723]

Tseng YC, et al. Lipid-calcium phosphate nanoparticles for delivery to the lymphatic system and SPECT/CT imaging of lymph node metastases. Biomaterials. 2014; 35:4688–4698. [PubMed: 24613050]

Uchiyama S, et al. Role of the standardized uptake value of 18-fluorodeoxyglucose positron emission tomography-computed tomography in detecting the primary tumor and lymph node metastasis in colorectal cancers. Surg. Today. 2012; 42:956–961. [PubMed: 22711186]

Uren RF. SPECT/CT Lymphoscintigraphy to locate the sentinel lymph node in patients with melanoma. Ann. Surg. Oncol. 2009; 16:1459–1460. [PubMed: 19363583]

Uren RF, et al. SPECT/CT scans allow precise anatomical location of sentinel lymph nodes in breast cancer and redefine lymphatic drainage from the breast to the axilla. Breast. 2012; 21:480–486. [PubMed: 22153573]

Vakoc BJ, et al. Three-dimensional microscopy of the tumor microenvironment in vivo using optical frequency domain imaging. Nat. Med. 2009; 15:1219–1223. [PubMed: 19749772]

van der Pas MH, et al. Laparoscopic sentinel lymph node identification in patients with colon carcinoma using a near-infrared dye: description of a new technique and feasibility study. J. Laparoendosc. Adv. Surg. Tech. A. 2013; 23:367–371. [PubMed: 23477368]

van der Vorst JR, et al. Optimization of near-infrared fluorescent sentinel lymph node mapping in cervical cancer patients. Int. J. Gynecol. Cancer. 2011; 21:1472–1478. [PubMed: 22027751]

van der Vorst JR, et al. Randomized comparison of near-infrared fluorescence imaging using indocyanine green and 99(m) technetium with or without patent blue for the sentinel lymph node procedure in breast cancer patients. Ann. Surg. Oncol. 2012; 19:4104–4111. [PubMed: 22752379]

van der Vorst JR, et al. Near-infrared fluorescence sentinel lymph node mapping of the oral cavity in head and neck cancer patients. Oral Oncol. 2013a; 49:15–19. [PubMed: 22939692]

van der Vorst JR, et al. Dose optimization for near-infrared fluorescence sentinel lymph node mapping in patients with melanoma. Br. J. Dermatol. 2013b; 168:93–98. [PubMed: 23078649]

Vercellino L, et al. Role of SPECT/CT in Sentinel Lymph Node Detection in Patients With Breast Cancer. Clin. Nucl. Med. 2014; 39:431–436. [PubMed: 23877520]

Vermeeren L, et al. Value of SPECT/CT for detection and anatomic localization of sentinel lymph nodes before laparoscopic sentinel node lymphadenectomy in prostate carcinoma. J. Nucl. Med. 2009; 50:865–870. [PubMed: 19443579]

von Andrian UH. Intravital microscopy of the peripheral lymph node microcirculation in mice. Microcirculation. 1996; 3:287–300. [PubMed: 8930886]

von der Weid PY. Lymphatic myogenic constriction - how lymphatic vessels pump lymph uphill. J. Physiol. 2013; 591:391–392. [PubMed: 23322290]

Wada H, et al. Lymph node staging by endobronchial ultrasound-guided transbronchial needle aspiration in patients with small cell lung cancer. Ann. Thorac. Surg. 2010; 90:229–234. [PubMed: 20609781]

Wagner T, et al. Fluorodeoxyglucose positron emission tomography fails to detect distant metastases at initial staging of melanoma patients with metastatic involvement of sentinel lymph node. Br. J. Dermatol. 2011; 164:1235–1240. [PubMed: 21332457]

Weiler M, et al. Sensitivity analysis of near-infrared functional lymphatic imaging. J. Biomed. Opt. 2012; 17:066019. [PubMed: 22734775]

Weissleder R, Thrall JH. The lymphatic system: diagnostic imaging studies. Radiology. 1989; 172:315–317. [PubMed: 2748809]

Wen Z, et al. The lymphoscintigraphic manifestation of 99mTc-dextran lymphatic imaging in primary intestinal lymphangiectasia. Nucl. Med. Commun. 2014; 35:493–500. [PubMed: 24488065]

Wu F, et al. Noninvasive real-time fluorescence imaging of the lymphatic uptake of BSA-IRDye 680 conjugate administered subcutaneously in mice. J. Pharm. Sci. 2012; 101:1744–1754. [PubMed: 22262501]

Xu N, et al. Integrated positron emission tomography and computed tomography in preoperative lymph node staging of non-small cell lung cancer. Chin. Med. J. (Engl.). 2014; 127:607–613. [PubMed: 24534208]

Yang Y, Oliver G. Development of the mammalian lymphatic vasculature. J. Clin. Invest. 2014; 124:888–897. [PubMed: 24590273]

Yaniv K, et al. Live imaging of lymphatic development in the zebrafish. Nat. Med. 2006; 12:711–716. [PubMed: 16732279]

Yasufuku K, et al. Comparison of endobronchial ultrasound, positron emission tomography, and CT for lymph node staging of lung cancer. Chest. 2006; 130:710–718. [PubMed: 16963667]

Yasufuku K, et al. A prospective controlled trial of endobronchial ultrasound-guided transbronchial needle aspiration compared with mediastinoscopy for mediastinal lymph node staging of lung cancer. J. Thorac. Cardiovasc. Surg. 2011; 142:1393–400. e1. [PubMed: 21963329]

Yousefi S, et al. Label-free optical lymphangiography: development of an automatic segmentation method applied to optical coherence tomography to visualize lymphatic vessels using Hessian filters. J. Biomed. Opt. 2013; 18:86004. [PubMed: 23922124]

Zawieja DC. Contractile physiology of lymphatics. Lymphat. Res. Biol. 2009; 7:87–96. [PubMed: 19534632]

Zawieja SD, et al. Impairments in the intrinsic contractility of mesenteric collecting lymphatics in a rat model of metabolic syndrome. Am. J. Physiol. Heart Circ. Physiol. 2012; 302:H643–H653. [PubMed: 22159997]

Zhi Z, et al. Label-free 3D imaging of microstructure, blood, and lymphatic vessels within tissue beds in vivo. Opt. Lett. 2012; 37:812–814. [PubMed: 22378402]

Zhou Q, et al. Near-infrared lymphatic imaging demonstrates the dynamics of lymph flow and lymphangiogenesis during the acute versus chronic phases of arthritis in mice. Arthritis Rheum. 2010; 62:1881–1889. [PubMed: 20309866]

Zhou Z, et al. A dual-modal magnetic nanoparticle probe for preoperative and intraoperative mapping of sentinel lymph nodes by magnetic resonance and near infrared fluorescence imaging. J. Biomater. Appl. 2013; 28:100–111. [PubMed: 23812946]

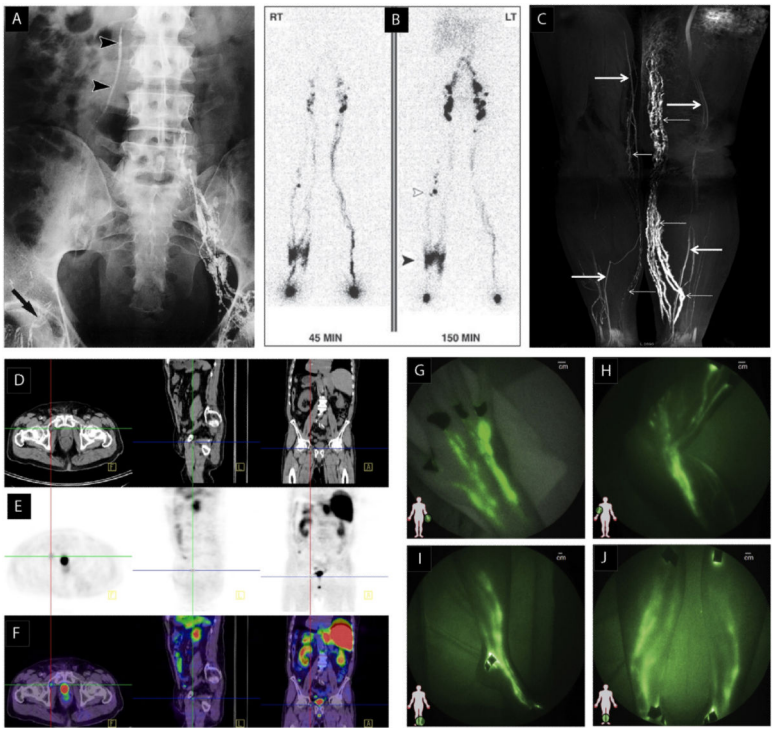

Fig. 1.

Imaging lymphatic vessels and lymph nodes in the clinic. (A) Lymphogram of a patient with lymphovenous shunt after surgery for right-sided inguinocrural hernia showing lack of lymph flow in the inguinocrural region (arrowheads) (Guermazi et al., 2003, reproduced with permission). (B) Lymphoscintigraphy of bilateral limb swelling. Lymph rerouting through the skin of right lower limb (solid arrowhead) and the deep lymphatics is apparent. Several popliteal nodes (open arrowhead) are visible. The left limb appears normal in this lymphoscintigraph (Burnand et al., 2011, reproduced with permission). (C) Coronal 3D MR lymphography image of the lower extremities obtained after subcutaneous injection of contrast material. Abnormal, dilated lymphatic vessels extend from the left calf to the inner thigh (small arrows). Some lymphatic vessels in the contralateral normal limb appear discontinuous (small arrows). Veins appear as linear structures with lower intensity (large arrows) (Lu et al., 2012). (D–F) PET-CT after radical prostatectomy. CT images are in (D), PET images 60 min after the administration of ^{18}F-choline are in (E) and merged PET-CT images are in (F). The high intensity spot in the PET scan is a small right inguinal lymph node with likely metastasis (F: transverse plane; L: saggital plane; A: coronal plane) (Fortuin et al., 2013). (G–J) Near infrared imaging of healthy lymphatics in normal subjects. Lymphatic vessels in (G) hand, (H) arm, (I) foot, ankle, and leg, and (J) lower legs. Black spots are covered injection sites (Rasmussen et al., 2009, reproduced with permission).

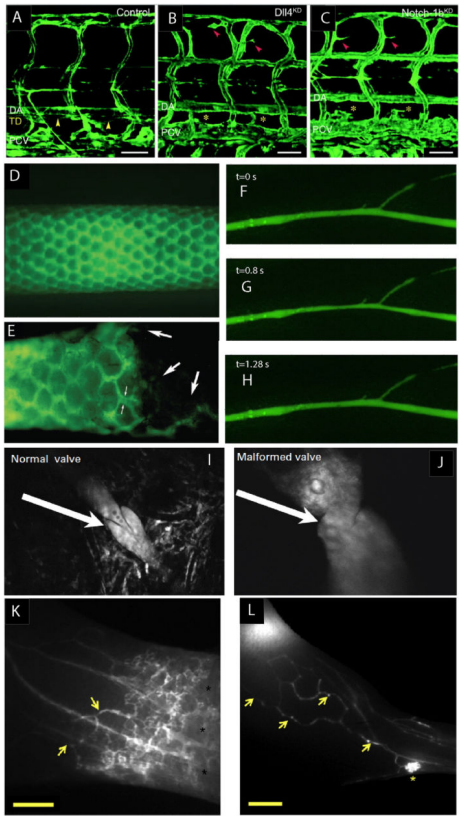

Fig. 2.

Lymphatic imaging in animal models. (A–C) Confocal microscopy of lymphatic development in the zebrafish. GFP signal comes from vessels in the Fli1:eGFPy1 embryo. Yellow arrowheads indicate normal thoracic duct in control embryos (A), which is absent in Dll4KD (B) and Notch-1bKD (C) embryos (Geudens et al., 2010, *reproduced with permission*). (D and E) Lymphatic vessels in a mouse tail imaged by fluorescence microscopy of FITC-dextran injected at the tip of the tail. Normal vasculature (D) is disrupted when a sarcoma is grown in the tail (E) (Leu et al., 2000, *reproduced with permission*). (F–H) Contraction of a collecting lymphatic vessel afferent to the popliteal lymph node in a mouse. A single pumping cycle lasting ~1.3 s is shown. The vessel was visualized by fluorescence microscopy of FITC-dextran injected in the footpad (Liao et al., 2011, *reproduced with permission*). (I and J) Lymphatic valve structures imaged using multiphoton microscopy identifies normal (I) and abnormal valves (J). Valve abnormalities are common around tumors (Hoshida et al., 2006). (K and L) Visualization of lymph flow redirection due to tumor growth in the hindlimb of a mouse using NIR imaging. (K) Normal uptake by collecting vessels and collateral flow (arrows). (L) Flow redirected through collecting vessel network (yellow arrows) toward the inguinal lymph node. Scale bar: 2 mm (Proulx et al., 2013a, *reproduced with permission*).

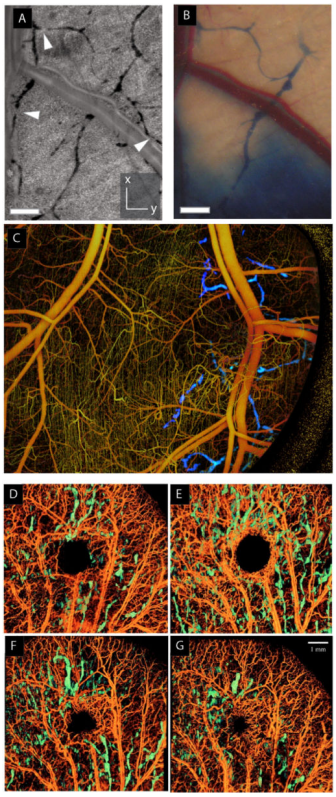

Fig. 3.

Emerging technologies for lymphatic imaging. (A–C) Optical frequency domain imaging of blood and lymphatic vessels. Lymphatic vessels appear as dark features with resolution comparable to traditional optical microscopy, but no contrast agent is required; thus, more vessels are detected by OFDI (A) than traditional lymphangiography (B). Blood vessels (yellow) and lymphatic vessels (blue) can be visualized in the same tissue with appropriate processing (C) (Vakoc et al., 2009). (D–G) Wound healing visualized by OCT imaging. Lymphatic vessels (green) and blood vessels at day 1 (D), day 8 (E), day 15 (F) and day 22 (G) after excision with a biopsy punch. (Yousefi et al., 2013, *reproduced with permission*).